

## Defluorination of Perfluoropropene Using $\text{Cp}^*_2\text{ZrH}_2$ and $\text{Cp}^*_2\text{ZrHF}$ : A Mechanism Investigation from a Joint Experimental–Theoretical Perspective

Eric Clot,<sup>†</sup> Claire Mégret,<sup>†</sup> Bradley M. Kraft,<sup>‡</sup> Odile Eisenstein,<sup>\*,†</sup> and William D. Jones<sup>\*,‡</sup>

Contribution from the Laboratoire de Structure et Dynamique des Systèmes Moléculaires et Solides (UMR 5636), Case Courrier 14, Université Montpellier 2, 34095 Montpellier Cedex 5, France, and Department of Chemistry, University of Rochester, Rochester, New York 14627

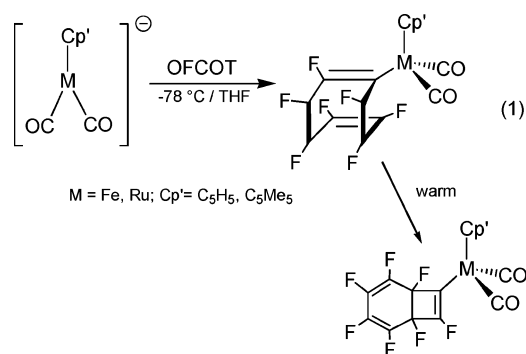
Received January 6, 2004; E-mail: odile.eisenstein@univ-montp2.fr; jones@chem.rochester.edu

**Abstract:**  $\text{Cp}^*_2\text{ZrH}_2$  (**1\***) ( $\text{Cp}^*$  = pentamethylcyclopentadienyl) reacts with perfluoropropene (**2**) to give  $\text{Cp}^*_2\text{ZrHF}$  (**3\***) and hydrodefluorinated products under very mild conditions. Initial C–F bond activation occurs selectively at the vinylic terminal position of the olefin to exchange fluorine for hydrogen. Subsequent hydrodefluorination leads to the formation of the *n*-propylhydride complex  $\text{Cp}^*_2\text{ZrH}(\text{CH}_2\text{CH}_2\text{CH}_3)$ , which can be cleaved with dihydrogen to give propane and **1\***. A theoretical study of the reaction of  $\text{Cp}_2\text{ZrH}_2$  ( $\text{Cp}$  = cyclopentadienyl) and  $\text{CF}_2=\text{CF}(\text{CF}_3)$  has been undertaken. Several mechanisms have been examined in detail using DFT(B3PW91) calculations and are discussed for this H/F exchange: (a) internal olefin insertion/ $\beta$ -fluoride elimination, (b) external olefin insertion/ $\beta$ -fluoride elimination, and (c) F/H metathesis from either an inside or outside approach. Of these, the first case is found to be energetically preferred. Selective defluorination at the terminal carbon has been shown to be favored over defluorination at the substituted and allylic carbons.

### Introduction

The mechanisms of carbon–fluorine bond activation in various substrates by  $\text{Cp}^*_2\text{ZrH}_2$  have been investigated for a wide variety of fluorocarbon substrates. Aliphatic fluorocarbons react to form  $\text{Cp}^*_2\text{ZrHF}$  and alkane by a radical chain mechanism.<sup>1</sup> Fluorobenzene reacts with  $\text{Cp}^*_2\text{ZrH}_2$  to form benzene,  $\text{Cp}^*_2\text{ZrHF}$ , and  $\text{Cp}^*_2\text{Zr}(\text{C}_6\text{H}_5)\text{F}$  via competing dual mechanisms involving (1) nucleophilic hydride addition/fluoride elimination and (2) initial ortho C–H activation,  $\beta$ -F elimination to give an intermediate benzyne complex, and insertion of the coordinated benzyne into the Zr–H bond.<sup>1</sup> Finally, non-perfluorinated alkenes containing allylic C–F bonds react to give hydrodefluorinated organic products and  $\text{Cp}^*_2\text{ZrHF}$  by an insertion/ $\beta$ -fluoride elimination mechanism.<sup>2</sup> Only a few studies have examined reactions with perfluoroolefins, where selective C–F activation could lead to selective formation of hydrofluorocarbon products.

Examples of reactions involving transition metal complexes and perfluorinated alkenes are relatively rare. Metal carbonyl anions such as  $[(\eta^5\text{-C}_5\text{R}_5)\text{M}(\text{CO})_2]^-$  ( $\text{M} = \text{Fe}$ ,  $\text{R} = \text{H}$ ;  $\text{M} = \text{Fe}$ ,  $\text{R} = \text{CH}_3$ ;  $\text{M} = \text{Ru}$ ,  $\text{R} = \text{H}$ ) react with octafluorocyclooctatetraene (OFCOT) to afford monosubstitution products with nucleophilic displacement of fluoride ion (eq 1). Further



warming of the  $\eta^1$ -heptafluorocyclooctatetraene complexes produces the bicyclic valence isomer complexes.<sup>3</sup> Similarly, Peterson et al. also saw nucleophilic displacement of fluoride in the reaction of  $\text{Cp}^*\text{Ir}(\text{PMe}_3)\text{HLi}$  with perfluoropropene.<sup>4</sup>  $\text{Me}_3\text{Sn-Mn}(\text{CO})_5$  reacts with  $\text{CF}_2=\text{CFH}$  photochemically to afford  $\text{CHF}=\text{CFMn}(\text{CO})_5$  and  $\text{Me}_3\text{SnF}$ . A mechanism was proposed involving olefin insertion to give  $\text{Me}_3\text{SnCFHCF}_2\text{Mn}(\text{CO})_5$  followed by fluoride migration to give the observed products.<sup>5</sup> Alternatively, the reaction may be viewed as a nucleophilic attack on the fluoroolefin by the  $[\text{Mn}(\text{CO})_5]^-$  anion. Wolczanski

<sup>†</sup> Université Montpellier 2.

<sup>‡</sup> University of Rochester.

(1) Kraft, B. M.; Lachicotte, R. J.; Jones, W. D. *J. Am. Chem. Soc.* **2001**, *123*, 10973.

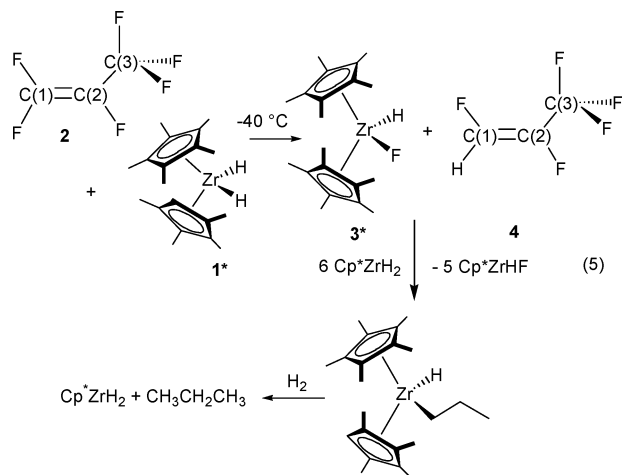
(2) Kraft, B. M.; Jones, W. D. *J. Am. Chem. Soc.* **2002**, *124*, 8681.

(3) Hughes, R. P.; Carl, R. T.; Doig, S. J.; Hemond, R. D.; Samkoff, D. E.; Smith, W. L.; Stewart, L. C.; Davis, R. E.; Holland, K. D.; Dickens, P.; Kashyap, R. P. *Organometallics* **1990**, *9*, 2732.

(4) Peterson, T. H.; Golden, J. T.; Bergman, R. G. *Organometallics* **1999**, *18*, 2005.

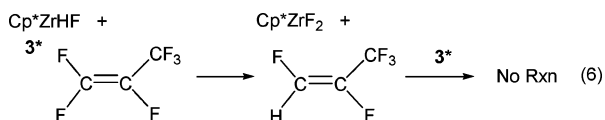
(5) Clark, H. C.; Tsai, J. H. *Inorg. Chem.* **1966**, *5*, 1407.





$\text{CH}_2\text{CH}_3\text{H}$  and traces (<5%) of unidentified fluorinated species were also detected. The reaction proceeds at  $-40\text{ }^\circ\text{C}$ , and no intermediates could be observed using low-temperature NMR spectroscopy, unlike reactions with nonperfluorinated olefins, which showed the intermediacy of both *iso*- and *n*-propyl insertion products.<sup>2</sup> Subsequent addition of a second equivalent of **1\*** produced more  $\text{Cp}^*_2\text{Zr}(\text{CH}_2\text{CH}_2\text{CH}_3)\text{H}$ , and no other fluorinated organic species were observed in appreciable quantities. Reaction of excess **1\*** (8 equiv) with perfluoropropene at room-temperature results in complete defluorination to produce a mixture of **3\***,  $\text{Cp}^*_2\text{Zr}(\text{CH}_2\text{CH}_2\text{CH}_3)\text{H}$ , and a small amount of  $\text{Cp}^*_2\text{ZrF}_2$  (eq 5). When the reaction was performed in the presence of 1.3 atm of  $\text{H}_2$  and an internal standard, propane was formed quantitatively based on  $\text{CF}_2=\text{CFCF}_3$ .

Reaction of **3\*** with  $\text{CF}_3\text{CF}=\text{CF}_2$  produced  $\text{Cp}^*_2\text{ZrF}_2$ , (*E*)- $\text{CFH}=\text{CFCF}_3$ , and a small amount (4%) of an unidentified organic species (eq 6). The reaction was slow at room



temperature, reaching 50% conversion after 3 days. In the presence of excess **3\***, no further reaction with (*E*)- $\text{CFH}=\text{CFCF}_3$  was observed.

**DFT Study of Mechanisms.** The above experiments reveal little about the mechanism of C–F cleavage since no intermediates are seen and since no labeling study is possible. For this reason, we have chosen to perform a detailed study with DFT calculations of  $\text{Cp}_2\text{ZrH}_2$ , **1**, ( $\text{Cp} = \eta^5\text{-C}_5\text{H}_5$ ), with  $\text{CF}_2=\text{CF}(\text{CF}_3)$ , **2**. Several pathways were examined (olefin insertion, F/H metathesis), and only one was found to be substantially preferred over the others. This pathway involves the approach of the olefin between the two hydrides (*internal*) to give an isopropyl hydride intermediately followed by a selective  $\beta$ -F elimination to give exclusively  $\text{Cp}_2\text{ZrHF}$ , **3**, and  $\text{CHF}=\text{CF}(\text{CF}_3)$ , **4**. This reaction is calculated to be strongly exergonic ( $\Delta E = -67.4\text{ kcal mol}^{-1}$ ). Below we describe this pathway in detail as well as pathways involving the external approach of the olefin, the Zr-alkyl intermediates prior to  $\beta$ -F elimination to analyze the regiochemistry, and the F/H metathesis pathway. In these calculations, all energies, unless otherwise stated, will be given with respect to separated reactants **1** plus **2**.

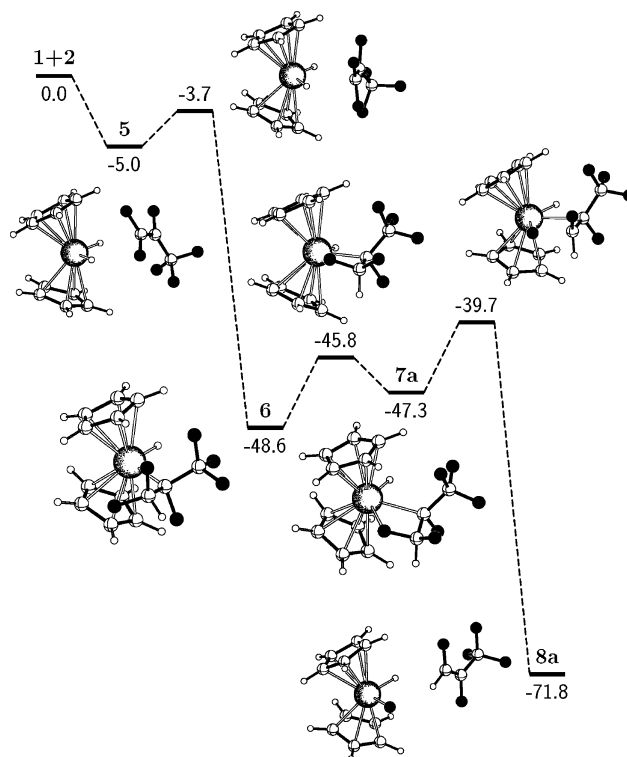


**Figure 1.** Energy profile ( $\text{kcal mol}^{-1}$ ) of the internal insertion/ $\beta$ -F elimination of  $\text{CF}_2=\text{CF}(\text{CF}_3)$ , **2**, in  $\text{Cp}_2\text{ZrH}_2$ , **1**.

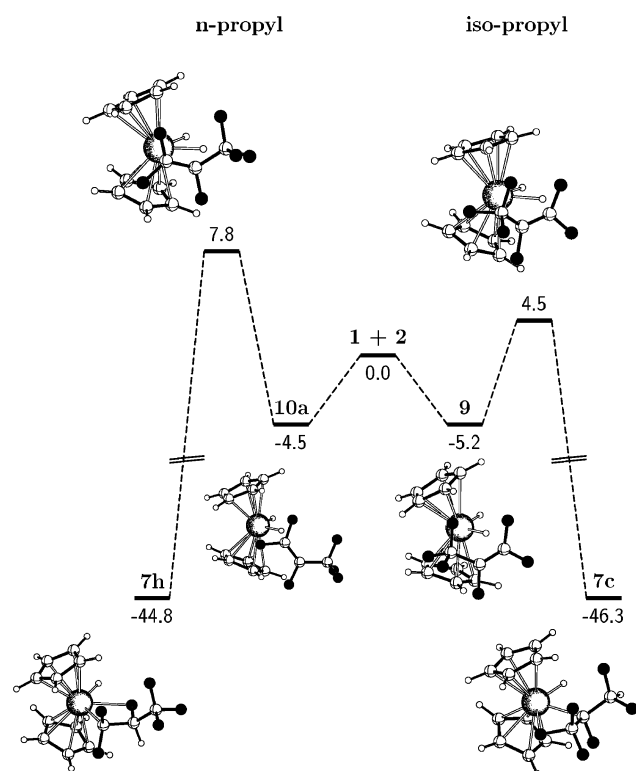
**(a) Preferred Pathway: Internal Insertion/ $\beta$ -F Elimination.** A weakly bound complex, **5**, is found between the hydridic Zr–H of  $\text{Cp}_2\text{ZrH}_2$ , **1**, and the terminal end C(1) of the electrophilic perfluoropropene, **2** ( $\text{H}\cdots\text{C}(1) = 2.886\text{ \AA}$ ). An adduct between Zr–H and C(2) has not been found to be a local minimum on the potential energy surface (PES) despite many attempts. In a very exothermic step, the complex with C(1) transforms into an isopropyl insertion product, **6**, with a very small barrier (Figure 1). In the intermediate **6**, the  $\alpha$ -F lies out of the plane of the wedge between the Cp ligands where it cannot interact with Zr because of the lack of an available empty orbital; the  $\beta$ -F is  $3.44\text{ \AA}$  from the metal center. This intermediate, however, does rearrange to form a new intermediate **7a** in which one of the  $\beta$ -F now interacts with Zr external to the C–Zr–H angle. It is interesting to note that the Zr–C–( $\text{CF}_2\text{H}$ ) angle closes from  $120.3^\circ$  in **6** to  $96.6^\circ$  in **7a**. At the same time, the  $\beta$  C–F bond in the  $\text{CF}_2\text{H}$  group lengthens from  $1.375\text{ \AA}$  to  $1.443\text{ \AA}$ , which puts the fluorine  $2.454\text{ \AA}$  from Zr. For reference, the C–F bond lengths in the  $\text{CF}_3$  group average  $1.35\text{ \AA}$ , while the Zr–F bond is  $1.934\text{ \AA}$  in **3**. From **7a**, an energy barrier of only  $7.6\text{ kcal mol}^{-1}$  is required to cleave the C–F bond and give a weak adduct **8a** of products  $\text{Cp}_2\text{ZrHF}$ , **3**, and (*E*)- $\text{CHF}=\text{CF}(\text{CF}_3)$ , **4**, with an overall release of energy of  $71.8\text{ kcal mol}^{-1}$ . The bond dissociation energy of **8a** into **3** and **4** is small ( $4.4\text{ kcal mol}^{-1}$ ).

**(b) External Insertion/ $\beta$ -F Elimination.** The above discussion describes the internal attack of the olefin between the hydride ligands. We have also examined attack of the olefin in the wedge but external to the two hydrides. The interaction of the olefin external to the two hydrides is favorable for only one of the two regiochemistries for the  $\text{CF}_3$  group (C(1)  $2.761\text{ \AA}$  from the hydride and C(2)  $4.650\text{ \AA}$  from Zr) to give **9** as a weak adduct between Zr–H and C(1) with a stabilization energy

**Table 1.** Selected Geometrical Parameters (Distance in Å, Angles in Degrees) and Energies (kcal mol<sup>-1</sup>) for the Alkyl Intermediates, **7**, with  $\beta$ -F Interaction and the Corresponding Transition States for  $\beta$ -F Elimination

	Zr-C <sub><math>\alpha</math></sub>	C <sub><math>\alpha</math></sub> -C <sub><math>\beta</math></sub>	C <sub><math>\beta</math></sub> -F <sub><math>\beta</math></sub>	Zr...F <sub><math>\beta</math></sub>	Zr-C <sub><math>\alpha</math></sub> -C <sub><math>\beta</math></sub>	C <sub><math>\alpha</math></sub> -C <sub><math>\beta</math></sub> -F <sub><math>\beta</math></sub>	Zr-C <sub><math>\alpha</math></sub> -C <sub><math>\beta</math></sub> -F <sub><math>\beta</math></sub>	$\Delta E^a$
<b>7a</b>	2.427	1.502	1.443	2.454	96.6	105.3	-17.3	-47.3
<b>7b</b>	2.421	1.516	1.442	2.492	98.8	104.6	-12.0	-47.9
<b>7c</b>	2.405	1.506	1.427	2.543	99.0	105.3	19.2	-46.3
<b>7d</b>	2.445	1.510	1.409	2.636	101.1	104.5	21.0	-49.4
<b>7e</b>	2.456	1.497	1.426	2.506	96.9	104.4	23.3	-48.7
<b>7f</b>	2.454	1.514	1.400	2.616	99.3	105.9	20.6	-44.8
<b>7g</b>	2.356	1.528	1.392	3.409	124.1	109.5	-17.3	-44.4
<b>7h</b>	2.437	1.526	1.425	2.492	99.1	103.9	9.7	-44.8
<b>TS7a-8a</b>	2.621	1.409	1.793	2.181	90.9	107.0	-5.6	-39.7
<b>TS7b-8b</b>	2.610	1.408	1.787	2.188	91.5	106.9	0.2	-41.7
<b>TS7c-8c</b>	2.591	1.407	1.850	2.167	93.2	103.9	7.9	-37.0
<b>TS7d-8d</b>	2.811	1.402	1.794	2.171	88.2	106.3	12.6	-36.1
<b>TS7e-8e</b>	2.812	1.399	1.789	2.159	87.0	106.9	14.8	-37.3
<b>TS7f-8f</b>	2.834	1.404	1.845	2.135	88.3	104.8	12.7	-29.5
<b>TS7g-8g</b>	2.524	1.410	1.756	2.230	92.8	107.3	-6.0	-34.0
<b>TS7h-8h</b>	2.724	1.399	1.776	2.202	89.8	108.1	-1.8	-29.0

<sup>a</sup> The energies are given with respect to separated reactants **1** plus **2**.

**Figure 2.** Energy profile (kcal mol<sup>-1</sup>) of the external insertion of CF<sub>2</sub>=CF(CF<sub>3</sub>), **2**, in Cp<sub>2</sub>ZrH<sub>2</sub>, **1**.

of 5.2 kcal mol<sup>-1</sup> similar to that for **5** (Figure 2). From intermediate **9**, however, a barrier of 9.7 kcal mol<sup>-1</sup> must be overcome to insert the olefin into the Zr-H bond and form a  $\beta$ -fluoride bound fluoroalkyl complex such as **7c**. From **7c**, an energy barrier of 9.3 kcal mol<sup>-1</sup> is required to cleave the C-F bond and give a weak adduct **8c** of products Cp<sub>2</sub>ZrHF, **3**, and CF<sub>2</sub>=CF(CHF<sub>2</sub>) with an overall release of energy of 62.3 kcal mol<sup>-1</sup> (not shown in Figure 2). The external pathway produces an allylic defluorinated olefin, not observed experimentally, and is associated with an higher energy barrier.

The other regiochemistry for external attack would put the less electrophilic C(2) center close to the hydride. This interaction is not strong enough to create an adduct similar to **9** and consequently the olefin slides to build the preferred interaction

between C(1) and H. Thus adduct **10a** corresponds to an external interaction of F-C(1) and Zr-H (Zr...F = 4.251 Å and H...C(1) = 2.798 Å). Compound **10a** must surmount a barrier of 12.3 kcal mol<sup>-1</sup> to produce the *n*-propyl derivative with a  $\beta$ -F interaction *internal* to the H-Zr-C angle such as **7h**.  $\beta$ -F elimination from **7h** is associated with a 15.8 kcal mol<sup>-1</sup> barrier and would lead to Cp<sub>2</sub>ZrHF + CF<sub>2</sub>=CHCF<sub>3</sub> which is not observed (not shown in Figure 2).

#### (c) Zr-Alkyl Isomers and Regiochemistry of Elimination.

In total, six Zr-isopropyl intermediates (**7a-f**) and two *n*-propyl isomers (**7g-h**) have been located on the PES (Figure 3 and Table 1). These isomers represent all possible insertion intermediates with a  $\beta$ -F interaction.<sup>26</sup> The  $\beta$ -F elimination from these isomers would lead to F/H substitution at any of the three carbons of the perfluoropropene. While the energies of the isopropyl isomers (**7a-f**) vary only over a range of 4.6 kcal mol<sup>-1</sup> (from -44.8 kcal mol<sup>-1</sup> to -49.4 kcal mol<sup>-1</sup> compared to **1** + **2**) where -49.4 kcal mol<sup>-1</sup> is the lower energy of intermediate **7** (**7d**, Table 1) and -44.8 kcal mol<sup>-1</sup> the highest energy (**7f**, Table 1), the energies of the associated transition states for  $\beta$ -fluorine elimination vary over a larger range (12.2 kcal mol<sup>-1</sup>, Table 1). The energy barriers for formation of the (*E*), via **TS7a-8a**, and (*Z*), via **TS7b-8b**, isomers of CHF=CF(CF<sub>3</sub>) are the lowest and differ by only 2 kcal mol<sup>-1</sup> with **TS7b-8b** being lower (Table 1). C-F activation at the allylic carbon C(3) has been shown to be associated with a less unfavorable transition state (**TS7c-8c**) only 4.7 kcal mol<sup>-1</sup> above the most favorable transition state. Substitution at C(2) from the less stable *n*-propyl complex **7g** requires crossing of the transition state (**TS7g-8g**) with an energy barrier of 9.6 kcal mol<sup>-1</sup>. The transition state for formation of the *n*-propyl **7g** from the isopropyl **7a** has also been located and is associated with a very high energy barrier (41.0 kcal mol<sup>-1</sup>), thus ruling out isomerization as a means of interconverting branched and linear products. The lack of observation of CF<sub>2</sub>=CH(CF<sub>3</sub>) is consistent with the higher energies of this energy profile. Therefore regardless of the way the Zr-isopropyl complexes **7a-f** are reached, the most favorable  $\beta$ -F elimination corresponds to F/H substitution at the terminal C(1) center.

(26) For **7c** and **7f**, where the  $\beta$ -F interaction is within the CF<sub>3</sub> group, rotamers of the CF<sub>2</sub>H group have been ignored.

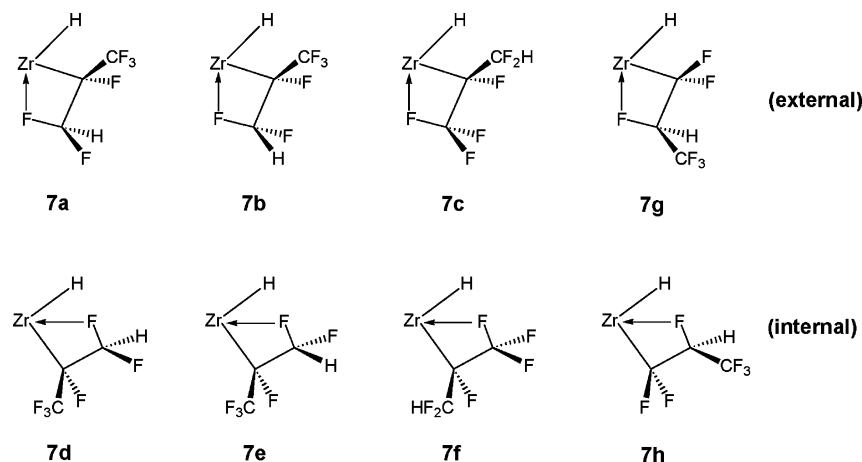


Figure 3. Structures of the alkyl isomers of species 7. See Table 1 for selected geometrical parameters and relative energies.

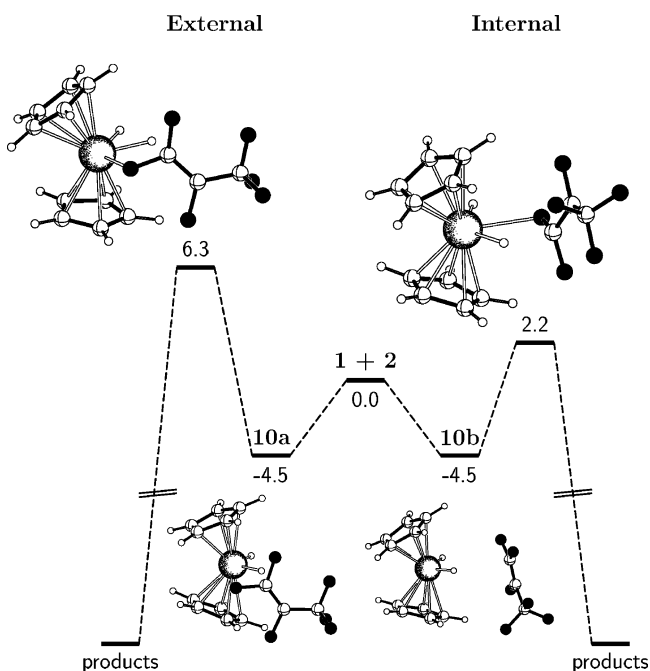


Figure 4. Energy profile ( $\text{kcal mol}^{-1}$ ) of the internal (right) and external (left) metathesis pathways of  $\text{CF}_2=\text{CF}(\text{CF}_3)$ , **2**, in  $\text{Cp}_2\text{ZrH}_2$ , **1**.

**(d) Metathesis Pathways.** The metathesis pathways involving internal and external four-center reactions of the  $\text{Zr}-\text{H}/\text{F}-\text{C}$  bonds were also investigated. As before adducts are formed, **10a** and **10b**, still involving only the hydride and the electrophilic carbon C(1) with an energy stabilization of 4–5  $\text{kcal mol}^{-1}$  and therefore rather similar to the previously located adducts (Figure 4). Concerted transition states for H/F exchange are located at either 6.7 or 10.8  $\text{kcal mol}^{-1}$  above the adducts, respectively. These pathways are therefore also less favored than the internal insertion/ $\beta$ -F elimination pathway.

## Discussion

Olefins are well known to insert into the  $\text{Zr}-\text{H}$  bond. Considering the multiple substitutions in perfluoropropene, it is not obvious which direction will be preferred nor if an insertion mechanism will be favored at all. Calculations over a variety of starting geometries support the idea that it (i) is largely exergonic, (ii) occurs with a low barrier, (iii) is selective in favor of the isopropyl product, and (iv) is selective to formation of the  $\text{CHF}=\text{CF}(\text{CF}_3)$  product.

The large energy of stabilization resulting from the hydrozirconation of the perfluorinated propene can be accounted for in terms of the strengths of the bonds that are made and broken. In the conversion of **5** to **6**, a  $\text{C}-\text{H}$  and a  $\text{Zr}-\text{C}$   $\sigma$  bond are made at the expense of a  $\text{Zr}-\text{H}$  bond and a  $\text{C}=\text{C}$   $\pi$  bond. Values for the three first bond energies can be estimated from experimental determination and are, respectively, around 106, 62, and 77  $\text{kcal mol}^{-1}$  for the  $\text{Cp}_2\text{Zr}$  compounds.<sup>27</sup> The  $\text{C}-\text{C}$   $\pi$  bond energy is expected to be very small as evidenced from the dramatic decreases of the total  $\text{C}=\text{C}$  energy with increasing number of F substituents:  $\text{CH}_2=\text{CH}_2$  (172  $\text{kcal mol}^{-1}$ ) vs  $\text{CF}_2=\text{CF}_2$  (76.3  $\text{kcal mol}^{-1}$ )<sup>28</sup> which accounts for the large negative reaction energy for **1** + **2** into **6** (–48.6  $\text{kcal mol}^{-1}$ ). Independent calculations of bond energies for  $\text{Zr}-\text{H}$  in  $\text{Cp}_2\text{ZrH}_2$  (70.5  $\text{kcal mol}^{-1}$ ),  $\text{Zr}-\text{C}$  in **6** (69.1  $\text{kcal mol}^{-1}$ ),  $\text{C}-\text{H}$  from  $\text{H}-\text{CF}_2\text{CFH}(\text{CF}_3)$  (105.8  $\text{kcal mol}^{-1}$ ), and  $\pi$   $\text{C}=\text{C}$  from the energy of hydrogenation of  $\text{CF}_2=\text{CF}(\text{CF}_3)$  (55.8  $\text{kcal mol}^{-1}$ ) highlight the role of the weakness of the  $\text{C}=\text{C}$   $\pi$  bond energy in driving down the reaction energy of **1** + **2** into **6**. This leads to the conclusion that while olefins are readily hydrozirconated, reactions with perfluoroolefins should be even more favorable.

The perfluoropropene **2** has a strongly asymmetric charge distribution in the carbon centers. AIM charges are calculated to be +1.2, +0.7, and +1.8 on C(1), C(2), and C(3), respectively.<sup>29</sup> The strong electrophilicity of C(1) accounts for the formation of internal encounter complex **5** where the  $\text{Zr}-\text{H}$  interacts with the terminal C. From this complex, the olefin slides slightly toward the hydride in crossing a low energy reactant-like transition state. An external complex of the olefin can also form. However in both orientations of the  $\text{CF}_3$  group, steric interactions in the transition state reveal that the carbon forming the incipient  $\text{Zr}-\text{C}$  bond (in the narrow part of the wedge) is further away from the metal than the carbon that will receive the hydrogen. These steric interactions would be expected to be exacerbated in the  $\text{Cp}^*\text{Zr}$  systems, accounting for the higher barrier to external insertion in these pathways.

The asymmetric charge distribution in the olefin **2** also accounts for the regioselective formation of the isopropyl product **6**. In the absence of an asymmetric charge distribution

(27) Simões, J. A. M.; Beauchamp, J. L. *Chem. Rev.* **1990**, *90*, 629.

(28) Bond Strengths in Polyatomic Molecules. *CRC Handbook of Chemistry and Physics*, 63rd ed. Weast, R. C., Ed.; CRC Press: Boca Raton, FL, 1983; p F-198.

(29) Bader, R. F. W. *Atoms in molecules: a quantum theory*; Clarendon Press: Oxford, 1990.

as in  $\text{CH}_2=\text{CH}(\text{CF}_3)$  ( $\Delta q = 0.01$  from AIM charges), a mixture of isopropyl and *n*-propyl insertion isomers is obtained.<sup>2</sup> Furthermore, from intermediate **7a**, the barrier to formation of the *n*-propyl isomer **7g** has been calculated to be greater than 40 kcal mol<sup>-1</sup>, ruling out isomerization as a means of interconverting branched and linear products.

The isopropyl complex **6**, which has no noticeable  $\alpha$ - or  $\beta$ -F interaction with the metal, is the preferred initial insertion product and thus needs to isomerize to other isopropyl intermediates with  $\beta$ -F interactions to give the Zr–F bond and the mono-defluorinated olefin products. Intermediates **7** all display  $\beta$ -fluorine interactions but are essentially at the same energy as **6** due to the ring strain introduced in the four-membered ring, mostly by closing of the Zr–C(1)–C(2) angle. The strength of the Zr $\cdots$ F interaction in **7** is also indicated by the almost equivalent Zr–C and Zr $\cdots$ F distances (Table 1). The six different isomers that have been selected are all within 4.6 kcal mol<sup>-1</sup>. The barriers for  $\beta$ -fluorine elimination from the isopropyl intermediates span an energy range of 12.2 kcal mol<sup>-1</sup> (Table 1). Since the  $\beta$ -fluorine bound isomers **7** interconvert rapidly with one another as demonstrated by the energy barrier of 2.8 kcal mol<sup>-1</sup> for **6** into **7a** (Figure 1), the major product would be determined by the Curtin–Hammett principle. The transition states for formation of  $\text{F}_2\text{C}=\text{CHCF}_3$  (**TS7g-8g**) and of  $\text{F}_2\text{C}=\text{CFCF}_2\text{H}$  (**TS7c-8c**) are at higher energies than those for forming  $\text{HFC}=\text{CFCF}_3$  (Table 1). The high activation barrier for  $\beta$ -F elimination at  $\text{CF}_3$  rather than at  $\text{CF}_2\text{H}$  is consistent with the increased C–F bond energy with increased F substitution at the central carbon (compare **7c** to **7a** or **7b**, Table 1). Furthermore the product  $\text{CF}_2=\text{CF}(\text{CF}_2\text{H})$  is the least stable of all possible products resulting from F/H substitution from perfluoropropene (10 kcal mol<sup>-1</sup> above (*E*)- $\text{CHF}=\text{CF}(\text{CF}_3)$ ). The higher barrier for  $\beta$ -F elimination at the substituted C(2) center does not follow from the trend in relative energies of (*E*)- $\text{CHF}=\text{CF}(\text{CF}_3)$  and  $\text{CF}_2=\text{CH}(\text{CF}_3)$  since the latter is more stable by 13.0 kcal mol<sup>-1</sup>. In summary, the F/H substitution at C(2) is disfavored because the lowest activation barrier for insertion of  $\text{CF}_2=\text{CF}(\text{CF}_3)$  corresponds to the formation of the isopropyl intermediates and the isopropyl  $\rightarrow$  *n*-propyl transformation has a high energy barrier; the F/H substitution at C(3) is disfavored by the higher energy associated with  $\beta$ -F elimination at  $\text{CF}_3$  compared to  $\text{CF}_2\text{H}$ . The first carbon to be defluorinated is thus C(1).

The selective formation of the (*E*) stereochemistry in the  $\text{CHF}=\text{CF}(\text{CF}_3)$  product is somewhat more complicated to account for. Experimentally the (*E*) isomer dominates which does not follow the relative energies of products, since (*Z*)- $\text{CFH}=\text{CF}(\text{CF}_3)$  is 1.8 kcal mol<sup>-1</sup> more stable than the (*E*) isomer. This means that the paths for production of these two isomers must be very similar with some marginal preference for formation of the (*E*) isomer. The calculations have identified two paths with very similar energy profiles, one leading to the (*E*) isomer (passage through **TS7a-8a**) and the other to the (*Z*) isomer (passage through **TS7b-8b**). A more precise calculation of the relative production of the two products would require calculations of the real systems including Cp\* in place of Cp.

The Zr-alkyl complexes with an internal  $\beta$ -F interaction (e.g., **7d**, **7e**) are generally more stable than those with an external  $\beta$ -F interaction (e.g., **7a**, **7b**). It is clearly preferable to put the stronger bond (M–C) at the outside and the weak bond (F $\rightarrow$

Zr) inside. The same rationale also accounts for the lower energy barrier for  $\beta$ -F elimination at the outside position. In the transition state, the Zr–F bond is well advanced and its formation is the main driving force for the reaction. Putting F where the incipient Zr–F bond would be stronger is thus preferred. Concomitantly, it is energetically less demanding to put the Zr–C bond at the coordination site where it is weakened. These results are consistent with the preference for internal insertion of the olefin.

It is interesting to note that the pathways for H/F metathesis via complexes **10a** and **10b** are not associated with particularly high barriers ( $\sim 10$  kcal mol<sup>-1</sup>). These barriers are in fact similar to those for  $\beta$ -fluorine elimination from complex **7**. The reason these metathesis pathways can be excluded is that the first step for the insertion/elimination has a barrier of only 2.3 kcal mol<sup>-1</sup> and is therefore strongly favored. Furthermore, the large exothermicity associated with the formation of the alkyl complexes permits the  $\beta$ -F elimination transition state to be considerably below the energy of the separated reagents. The energy realized in the insertion step could be used to carry the complex all the way to products over the  $\sim 10$  kcal mol<sup>-1</sup> barrier for  $\beta$ -F elimination, although, at the temperature in the experiment, there is sufficient thermal energy to surmount the barrier. These results suggest that, in a multistep process for an overall exothermic pathway, there may be some benefit in starting the reaction path with a step having the lowest barrier. This will result in the energy profile rising the least above the energy of the initial reactants.

It is interesting to compare and contrast these results with those of Caulton et al. on the reaction of  $\text{CH}_2=\text{CHF}$  with  $\text{Cp}_2\text{-ZrHCl}$ .<sup>24</sup> First, the overall reaction coordinate is very similar and an insertion/ $\beta$ -F elimination pathway was found to be favored. Second, while no adduct with vinyl fluoride was found prior to insertion, the reaction employing  $\text{Cp}_2\text{ZrH}_2$  with perfluoropropene shows evidence for adduct formation via a hydride–olefin interaction. This is likely due to the fact that  $\text{Cp}_2\text{ZrH}_2$  is more electron rich than  $\text{Cp}_2\text{ZrHCl}$  and that perfluoropropene is more electrophilic than vinyl fluoride. Third, both sets of calculations show evidence for  $\beta$ -fluoride interactions yet intermediate **7** is of comparable energy to intermediate **6** where this interaction is absent. In the  $\text{Cp}_2\text{Zr}(\text{Cl})(\text{CH}_2\text{CH}_2\text{F})$  case, the intermediate with the  $\beta$ -fluoride interaction is at higher energy than the intermediate without this interaction. This may be due to the fact that Cl is a  $\pi$ -donor and attenuates the Lewis acidity of Zr. The structures of the two alkyl complexes with  $\beta$ -F interactions are similar, and we believe that the Zr $\cdots$ F interaction is strong but is countered by the strain of the ring that is formed. Finally, the slower rate of reaction of  $\text{Cp}_2\text{ZrHCl}$  versus  $\text{Cp}^*\text{ZrH}_2$  can be attributed to the higher hydricity associated with dihydride versus hydrido-chloride, the greater donor ability of Cp\* versus Cp, and the greater electrophilicity of the olefin used. In this sense, the present calculations overestimate barriers, since they were done with Cp in place of Cp\*, although the calculated barriers for all paths are lower with  $\text{Cp}_2\text{ZrH}_2$  and  $\text{CF}_2=\text{CF}(\text{CF}_3)$  than with  $\text{Cp}_2\text{ZrHCl}$  and  $\text{CH}_2=\text{CHF}$ . Indeed, experiments show that use of  $\text{Cp}^*\text{ZrHF}$  results in slower rates.

The complete exchange of fluorine for hydrogen can be accomplished by successive repetitions of the pathways that have been described above. The fact that (*E*)- $\text{CHF}=\text{CF}(\text{CF}_3)$  is

observed to build up before subsequent reductions implies that the barrier height for the second reduction is higher than the first and all subsequent reductions. The reaction pathways calculated here are sufficiently facile to serve as potential mechanistic steps, but it is anticipated that the insertion/elimination pathway will continue to be favored. This notion is supported by calculations on the reaction of  $\text{Cp}_2\text{ZrH}_2$  with ethylene, which shows virtually no barrier to insertion.<sup>30</sup>

## Conclusions

Vinyl C–F bond exchange is extremely facile with the Zr–H bond of  $\text{Cp}^*_2\text{ZrH}_2$ . The first exchange occurs selectively at the terminal carbon C(1). DFT calculations strongly support an internal insertion of the olefin followed by  $\beta$ -F elimination over other pathways with the terminal substitution being preferred. The regiochemistry of the exchange, determined at the insertion step, is associated with the strong asymmetric charge distribution in the perfluoropropene olefin.

## Experimental Section

**General Considerations.** All manipulations were performed inside an  $\text{N}_2$ -filled Vacuum Atmospheres glovebox or on a high vacuum line. Cyclohexane, cyclohexane- $d_{12}$ , and toluene- $d_8$  (Cambridge) were dried and vacuum distilled from purple solutions of benzophenone ketyl. UHP grade  $\text{H}_2$  (Air Products) was purified by passage over activated 4 Å molecular sieves and MnO on vermiculite.<sup>31</sup> Perfluoropropene (Aldrich), was used as received. All liquids were degassed by the freeze–pump–thaw method.  $^1\text{H}$  and  $^{19}\text{F}$  NMR spectra were recorded using a Bruker Avance400 spectrometer.  $^{19}\text{F}$  NMR spectra were referenced to  $\alpha,\alpha,\alpha$ -trifluorotoluene (taken as  $\delta -63.73$  relative to  $\text{CFCl}_3$  with downfield chemical shifts taken to be positive).  $^{19}\text{F}$  NMR spectra were recorded at a minimum resolution of 0.5 Hz.  $\text{Cp}^*_2\text{ZrH}_2$  was prepared according to the literature procedures.<sup>32,33</sup>

**Reaction of 1 with Perfluoropropene.** A resealable NMR tube was charged with 30 mg (0.082 mmol) of  $\text{Cp}^*_2\text{ZrH}_2$  and dissolved in  $\text{C}_6\text{D}_{12}$ . The solution was freeze–pump–thaw degassed 3 times and with a 56-mL calibrated glass bulb, and 4 Torr (0.012 mmol) of perfluoropropene was condensed in the tube. The tube was thawed, shaken, and analyzed after 2 h at room temperature.  $^{19}\text{F}$  NMR analysis revealed formation of  $\text{Cp}^*_2\text{ZrHF}$  and a small amount of  $\text{Cp}^*_2\text{ZrF}_2$ . No other fluorinated organic species were observed. The  $^1\text{H}$  NMR spectrum revealed the formation of  $\text{Cp}^*_2\text{Zr}(n\text{-propyl})\text{H}$  and a small amount of propane. When the reaction was repeated using 1 equiv of perfluoropropene, the reaction mixture consisted primarily of (*E*)-1,2,3,3,3-

pentafluoropropene, unreacted perfluoropropene, and  $\text{Cp}^*_2\text{Zr}(\text{CH}_2\text{CH}_2\text{CH}_3)\text{H}$ . No other fluorocarbons were observed upon reaction with additional equivalents of  $\text{Cp}^*_2\text{ZrH}_2$ . For (*E*)-1,2,3,3,3-pentafluoropropene:  $^{19}\text{F}$  NMR ( $\text{C}_6\text{D}_{12}$ ):  $\delta -69.55$  (m, 3 F),  $-166.03$  (m, 1 F),  $-178.73$  (dm,  $J_{\text{trans F-F}} = 139$  Hz, 1 F).  $^1\text{H}$  NMR ( $\text{C}_6\text{D}_{12}$ ):  $\delta 7.11$  (dd,  $J_{\text{gem H-F}} = 70.7$  Hz). The chemical shifts and coupling constants match those reported.<sup>34</sup>

## Computational Details

All calculations were performed with the Gaussian 98 set of programs<sup>35</sup> within the framework of hybrid DFT (B3PW91).<sup>36</sup> The zirconium atom was represented by the relativistic effective core potential (RECP) from the Stuttgart group (12 valence electrons) and its associated basis set,<sup>37</sup> augmented by an *f* polarization function ( $\alpha = 0.875$ ).<sup>38</sup> A 6-31G(d,p) basis set<sup>39</sup> was used for all the remaining atoms. Full optimizations of geometry without any constraint were performed, followed by analytical computation of the Hessian matrix to confirm the nature of the located extrema as minima or transition states on the potential energy surface. The connection between reactants through the transition states was checked by optimizations from a slightly altered geometry of the transition state in both directions along the transition state vector.

**Acknowledgment.** The U.S. Department of Energy, Grant FG02-86ER13569 is gratefully acknowledged for their support of this work. The authors thank the CINES French national computing center for an allocation of computational time under the Grant x2002 08 22334.

**Supporting Information Available:** Detailed information on the reaction paths including coordinates of extrema. This material is available free of charge via the Internet at <http://pubs.acs.org>.

JA0499243

- (30) Calculations of olefin insertion into a Zr–H bond generally show low barriers. See ref 24 and Endo, J.; Koga, N.; Morokuma, K. *Organometallics* **1993**, *12*, 2777.  
 (31) Brown, T. L.; Dickerhoof, D. W.; Bafus, D. A.; Morgan, G. L. D. *Rev. Sci. Instrum.* **1962**, *33*, 491.  
 (32) Schock, L. E.; Marks, T. J. *J. Am. Chem. Soc.* **1988**, *110*, 7701.  
 (33) Eujen, R. *Inorg. Synth.* **1986**, *24*, 52.

- (34) Koroniak, H.; Palmer, K. W.; Dolbier, W. R.; Zhang, H. *Magn. Reson. Chem.* **1993**, *31*, 748.  
 (35) Frisch, M. J.; Trucks, G. W.; Schlegel, H. B.; Scuseria, G. E.; Robb, M. A.; Cheeseman, J. R.; Zakrzewski, V. G.; Montgomery, J. A.; Stratmann, R. E.; Burant, J. C.; Dapprich, S.; Millam, J. M.; Daniels, A. D.; Kudin, K. N.; Strain, M. C.; Farkas, O.; Tomasi, J.; Barone, V.; Cossi, M.; Cammi, R.; Mennucci, B.; Pomelli, C.; Adamo, C.; Clifford, S.; Ochterski, J.; Petersson, G. A.; Ayala, P. Y.; Cui, Q.; Morokuma, K.; Malick, D. K.; Rabuck, A. D.; Raghavachari, K.; Foresman, J. B.; Cioslowski, J.; Ortiz, J. V.; Baboul, A. G.; Stefanov, B. B.; Liu, G.; Liashenko, A.; Piskorz, P.; Komaromi, I.; Gomperts, R.; Martin, R. L.; Fox, D. J.; Keith, T.; Al-Laham, M. A.; Peng, C. Y.; Nanayakkara, A.; Gonzalez, C.; Challacombe, M.; Gill, P. M. W.; Johnson, B. G.; Chen, W.; Wong, M. W.; Andres, J. L.; Head-Gordon, M.; Replogle, E. S.; Pople, J. A. *Gaussian 98*, revision A11; Gaussian, Inc.: Pittsburgh, PA, 1998.  
 (36) (a) Becke, A. D. *J. Chem. Phys.* **1993**, *98*, 5648. (b) Perdew J. P.; Wang, Y. *Phys. Rev. B* **1992**, *82*, 284.  
 (37) Andrae, D.; Häussermann, U.; Dolg, M.; Stoll, H.; Preuss, H. *Theor. Chim. Acta* **1990**, *77*, 123.  
 (38) Ehlers, A. W.; Böhme, M.; Dapprich, S.; Gobbi, A.; Höllwarth, A.; Jonas, V.; Köhler, K. F.; Stegmann, R.; Veldkamp, A.; Frenking, G. *Chem. Phys. Lett.* **1993**, *208*, 111.  
 (39) Hariharan, P. C.; Pople, J. A. *Theor. Chim. Acta* **1973**, *28*, 213.